# Bis-phosphonates–ultra small superparamagnetic iron oxide nanoparticles: a platform towards diagnosis and therapy†

**Yoann Lalatonne,[ab] Céline Paris,[a] Jean Michel Serfaty,[c] Pierre Weinmann,[b] Marc Lecouvey[a] and Laurence Motte*[a]**

*Received (in Cambridge, UK) 1st February 2008, Accepted 3rd March 2008*
*First published as an Advance Article on the web 28th March 2008*
**DOI: 10.1039/b801911h**

**A new type of multifunctional magnetic nano-platform for diagnosis and therapy applications was designed using bis-phosphonate/carboxylic ligands.**

Superparamagnetic iron oxide[1] (SPIO) nanoparticles currently appear to be a more relevant MRI contrast agent than Gd chelates due to the high MR signal per unit of metal. Usually, they are prepared by an alkaline precipitation[2–4] of solutions containing iron(II) and iron(III) salts, thermal decomposition of the iron precursor[5–11] or synthesis in micellar system.[12–14] To prevent aggregation of the particles and to endow them with pharmacological properties, the surface is coated with hydrophilic polymers such as dextran or polyethylene glycol (PEG).[15,16] However the polymer coating significantly increases their overall size and therefore may limit their tissue distribution, penetration, and metabolic clearance. One other way of performing this is coating the surface with bifunctional molecules that are hydrophilic on one end and bind to the nanocrystal surface with the other end. Many different crosslinkers are used such as carboxymethyl dextran,[17] amino PEG,[18] mercapto carbonic acid.[8,19] Moreover the carboxyl, amine and thiol hydrophilic end groups can be used to conjugate biological molecules to provide a location for the vector enhancing MR signal in pathological areas or tissues.[20,21] Usually, the fixation site on an iron core is carboxylate. Only limited recent reports[9,10,22–27] have investigated other anchoring agents as sulfonate, phosphate and phosphonate. A strong interaction between the inorganic core and the phosphonic moiety is reported[10,25] and the more interesting fixation moiety seems to be bisphosphonate.[24]

With respect to bisphosphonate's biological activity, this class of compounds exhibits a powerful binding affinity to bones and is routinely used in the treatment of bone resorption and other bone disorders like Paget's disease, osteoporosis, or tumor induced osteolysis.[28] Their biological activity can be modified by altering the structure of the two side chains on the carbon atom. The binding to bone mineral depends upon the P–C–P structure and is enhanced by including a hydroxyl group (hydroxyl methylene bisphosphonate HMBP), probably due to tridendate binding hydroxyl substituted bisphosphonates to calcium. Recent works on the coordination ability of bisphosphonates have shown their very high efficiency in the binding of metal ions (iron).[29] The P–C–P bond system has low toxicity and high thermostability and is very resistant to enzymatic cleavage. Hence, the use of such compounds for the treatment of bone disorders, in addition to their iron chelating properties, is highly promising.

In this communication, we propose a new type of platform for the elaboration of a nano magnetic vector taking into account of previous considerations: maghemite nanoparticle surface are passivated using a bifunctional passivating agent such as 5-hydroxy-5,5-bis(phosphono)pentanoic acid (called HMBP–COOH in the text, Scheme 1). The HMBP function complexes the nanocrystal surface and carboxylate groups at the outer surface induce electrostatic repulsion between nanocrystals. A stable ferrofluid is obtained in a large concentration and pH range. The large number of COOH functionalities on the magnetic core of the particle can be used as precursor groups for the covalent coupling of biomolecules or fluorescence markers (Scheme 1). The feasibility of such a process is demonstrated by the coupling of amino fluorescein to the hybrid nanomaterial.

Maghemite $\gamma$-$Fe_2O_3$ nanocrystals were prepared as described previously[12–14] by soft chemistry. At the end of the synthesis, a solution of HMBP-COOH solubilized in water at pH 2 is added to the bare nanoparticle dispersion. The pH was then progressively increased to pH 7 by the addition of sodium hydroxide NaOH, thus achieving a stable dispersion of the

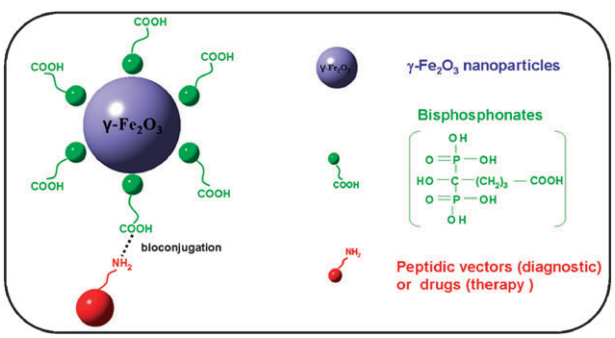


**Scheme 1** Nanomagnetic platform towards diagnosis and therapy.

[a] *Laboratoire BioMoCeTi UMR 7033 CNRS Université Paris 13, 74 Rue Marcel Cachin, 93017 Bobigny, France. E-mail: laurence.motte@smbh.univ-paris13.fr; Fax: (+33)148387625*
[b] *Service de Médecine Nucléaire, Hôpital Avicenne, 125 route de Stalingrad, 93009 Bobigny Cedex, France*
[c] *Service de Radiologie, Hôpital Bichat, 46 rue Henri Huchard, 75018 Paris Cedex, France*

† Electronic supplementary information (ESI) available: Details of experimental techniques and characterization. See DOI: 10.1039/b801911h

nanoparticles (details in ESI†). After dialysis, the dispersed solution is lyophilized. The powder is easily dispersed in water and the nanoparticles sols are stable over a broad range of pH (4–12) and concentration (over 40 wt%), in suitable ionic strength ($<0.6$ mol $L^{-1}$) and in various biological buffers such as PBS and Hepes (See ESI Fig. S1 and S2†). The TEM image (insert Fig. 1) of deposited nanocrystals indicates an average diameter and a polydispersity, respectively equal to 10 nm and 20%. Hence, as it was observed in previous work, with citrate and carboxylic acid used as coating agents, that the nanoparticles' size and polydispersity remain the same, whatever their coating.[13,14]

ATR-FTIR spectroscopy analysis show that the phosphonate groups are highly complexant compared to the carboxylate group (Fig. 1). For the free HMBP-COOH molecules (blue curve), the carboxylate ions present two characteristic bands[30] at 1546 and 1407 $cm^{-1}$ due to the asymmetric and symmetric carboxylate stretches, respectively. Within the P–O stretching region (1200–900 $cm^{-1}$), the spectrum exhibits two sharp peaks at 1153 and 982 $cm^{-1}$, assigned to P═O and P–OH, respectively.[31] The broad band at 1073 $cm^{-1}$ is characteristic for the vibrational mode for the $PO_3$ group.[32] Comparing the HMBP-COOH coated nanocrystals (red curve) with the free HMBP-COOH solution (blue curve), the carboxylate region (1600–1400 $cm^{-1}$) is unchanged and at the opposite end of the spectrum, the large changes observed within the P–O stretching region (1200–900 $cm^{-1}$) show that a strong interaction between the phosphonate headgroup and the $Fe_2O_3$ surface is present. These results are consistent with phosphonate binding to the oxide surface[10,25] and we can suggest that the Fe atoms within the particle surface are coordinated by oxygen atoms from the phosphonate groups.[33] Hence, ATR-FTIR analysis indicates that the HMBP group is highly complexant compared to the carboxylate group as opposed to reported results with bi functional ligands bearing a single phosphonate and carboxylic function.[9] This suggests a cooperative effect of the two phophonate and hydroxyl groups. Hence, the carboxylate groups lead to electrostatic repulsions between nanoparticles. Quantitative ATR-FTIR experiments (see ESI Fig. S3†) indicate a value of 1800 HMBP molecules per 10 nm nanoparticle, corresponding to 0.1 equivalents per Fe ion (around 0.3 per surface Fe ion).

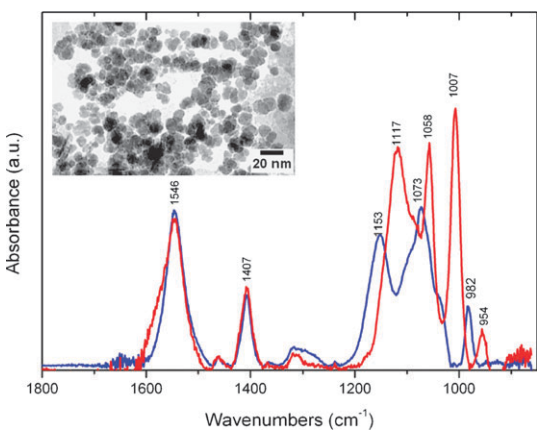


**Fig. 1** ATR-FTIR spectra of HMBP-COOH free molecules (blue curve) and HMBP coated nanoparticles (red curve), recorded at neutral pH, in $H_2O$ solutions and subtracted of $H_2O$ bands. Insert: transmission electron microscopy image taken of a nanoparticle solution at pH 7.

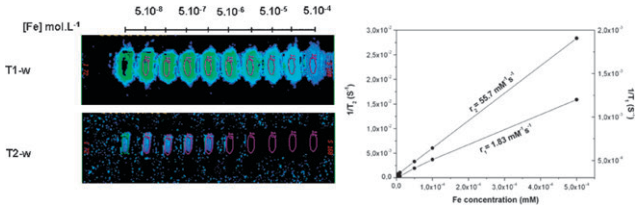


**Fig. 2** (a) $T_1$ weight MR images and $T_2$ weight MR images of aqueous solutions of as-synthesized nanoparticles at different Fe concentrations; (b) $T_1$ and $T_2$ relaxation rates ($1/T_1$, $1/T_2$) plotted against the Fe concentration for the various aqueous solutions.

To investigate the MR signal enhancement effects, the aqueous as-prepared nanoparticles at different Fe concentrations were measured on a clinical 1.5 T MRI scanner. As shown in Fig. 2a, both $T_1$ and $T_2$ weighted images change drastically in signal intensity with an increasing amount of nanoparticles, indicating that as synthesized nanoparticles generated MR contrast on both longitudinal ($T_1$) and transverse ($T_2$) proton relaxation times weighted sequences. Fig. 2b shows the relaxation rates $1/T_1$ and $1/T_2$ as a function of the iron concentration. The relaxation rates varied linearly with the iron concentration, as expected. The longitudinal $r_1$ and transverse $r_2$ relaxivities (corresponding to the slopes of the lines) are found to be 1.83 Fe $mM^{-1}$ $s^{-1}$ and 55.7 Fe $mM^{-1}$ $s^{-1}$, respectively. Such values for $r_1$ and $r_2$ suggest that HMBP coated nanoparticles can act as both $T_1$ and $T_2$ contrast agents taking into account their small size, but seem to be more favourable as $T_2$ contrast agents due to their much larger $r_2$ value.

To demonstrate the use of HMPB-COOH coated nanocrystals as magnetic nano-platform, standard procedures were used to crosslink free carboxylic acid group with amino containing ligands such as amino fluorescein. Briefly, the as-synthesized nanocrystals were activated with soluble carbodimide (EDC), then the activated nanocrystals were reacted with amino fluorescein (details in ESI†). The fluorescein conjugated nanocrystals are then easily dispersed in water at pH 7. The efficiency of the coupling between amino fluorescein and the nanocrystals is evaluated using FTIR, fluorescence and UV-vis spectroscopies. The FTIR spectrum of amino-fluorescein coupled nanoparticles (see ESI Fig. S4†) presents a new peak at 1542 $cm^{-1}$ due to the bending δ(NH) vibration modes,[34] suggesting a chemical bonding between the carboxylic group (HMBP-COOH) and the amino group of the amino fluorescein. The emission spectrum of the magnetic fluorescent particles compared to free dye molecules in water at pH 7 is shown in Fig. 3a. The spectra are similar with a small red shift (5 nm) due to the amide groups or to the interaction between the dye and the nanocrystals. The peaks of the emission bands occurred at 515 nm for amino fluorescein and 520 nm for the amino fluorescein coupled nanoparticles. The molar ratio between the dye and the iron of the magnetic particles was deduced from the UV-vis absorption by

 

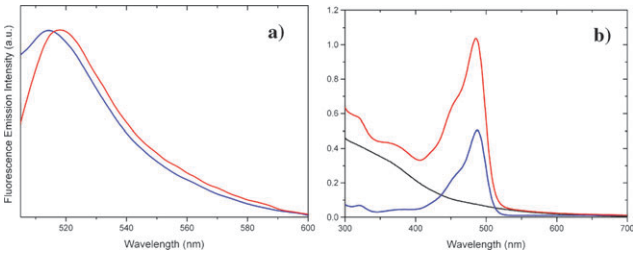


**Fig. 3** (a) Fluorescence emission spectra and (b) UV-vis absorption spectra, recorded at neutral pH and $\lambda_{exc}$ = 490 nm, of amino fluoroscein (blue curve), HMBP coated nanocrystals (black curve, only UV-vis absporption) and amino fluorescein coupled nanocrystals (red curve).

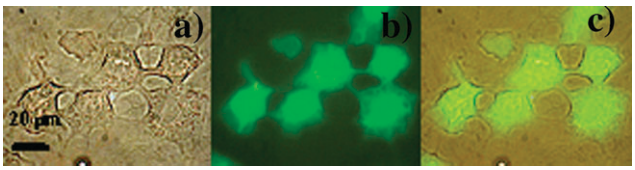


**Fig. 4** Observation of magnetic fluorescent nanoparticles in MDA-MB-231 living cells. (a) Transmission image, (b) fluorescence image and (c) overlay of transmission and fluorescence images.

comparison between the spectra of the as-synthesized nanocrystals, the conjugated nanocrystals and free aminofluorescein molecules (Fig. 3b). We found 590 dye molecules per particle, corresponding to 0.3 eq. HMBP. This ratio reduces slightly the electrostatic nanoparticle surface charges, nevertheless a stable ferrofluid is obtained. After chemical decomposition of the coupling the same ratio is found (details in ESI†).

HMBP coated nanocrystals and amino fluorescein coupled nanocrystals were incubated with MDA-MB-231 and MDA-MB-435 breast cancer cells precultured for 24 h, for various extra cellular iron concentrations up to 10 mmol $L^{-1}$. No cytoxicity was observed (see ESI Fig. S5†). Cellular uptake of the nanoparticles occurs by endocytosis: a representative TEM image (see ESI Fig. S6†) shows the nanocrystals' incorporation into an intracellular endocytotic vesicle. The fluorescence pattern shown in Fig. 4 demonstrates the capacity for combined fluorescent and magnetic labeling of living cells of the amino fluorescein coupled nanocrystals.

In conclusion, we have developed a new magnetic nano-platform using an highly iron-complexing agent (HMBP) containing a carboxylic acid group as a bio-conjugating precursor. To test the feasibility of such a nano-platform, fluorescein is coupled to the hybrid nanomaterial. Hence, a stable fluorescent ferrofluid is obtained and may serve as both a magnetic resonance contrast agent for MRI and an optical probe for fluorescence microscopy. We are now investigating the conjugation of this nano-platform with target or therapeutic molecules, focusing on two pathologies: cancer and atherosclerosis.

Our special thanks to Nicole Lièvre for her excellent technical assistance in transmission electron microscopy and to Odile Sainte Catherine for *in vitro* cell culture experiments and fluorescence microscopy.

## Notes and references

1 R. Lawaczeck, M. Menzel and H. Pietsch, *Appl. Organomet. Chem.*, 2004, **18**, 506–513.
2 C. C. Berry and A. S. G. Curtis, *J. Phys. D: Appl. Phys.*, 2003, **36**, R198.
3 T. Sugimoto and E. Matijevic, *J. Colloid Interface Sci.*, 1980, **74**, 227.
4 Y. S. Kang, S. Risbud, J. F. Rabolt and P. Stroeve, *Chem. Mater.*, 1996, **8**, 2209.
5 S. Sun and H. Zeng, *J. Am. Chem. Soc.*, 2002, **124**, 8204.
6 J. Park, E. Lee, N. M. Hwang, M. Kang, S. C. Kim, Y. Hwang, J. G. Park, H. J. Noh, J. Y. Kim, J. H. Park and T. Hyeon, *Angew. Chem., Int. Ed.*, 2005, **44**, 2819–2829.
7 T. Hyeon, S. Lee, J. Park, Y. Chung and H. B. Na, *J. Am. Chem. Soc.*, 2001, **123**, 12798.
8 Y. Jun, Y. M. Huh, J. S. Choi, J. H. lee, H. T. Song, S. Kim, S. Yoon, K. S. Kim, J. S. Shin, J. S. Suh and J. Cheon, *J. Am. Chem. Soc.*, 2005, **127**, 5732–5733.
9 H. T. Song, J. S. Choi, Y. M. Huh, S. Kim, Y. W. Jun, J. S. Suh and J. Cheon, *J. Am. Chem. Soc.*, 2005, **127**, 9992–9993.
10 K. V. P. M. Shafi, A. Ulman, X. Yan, N. L. Yang, C. Estournes, H. White and M. Rafailovich, *Langmuir*, 2001, **17**, 5093–5097.
11 J. Wan, W. Cai, X. Meng and E. Liu, *Chem. Commun.*, 2007, 5004.
12 A. T. Ngo and M. P. Pileni, *J. Phys. Chem. B*, 2001, **105**, 53.
13 Y. Lalatonne, L. Motte, V. Russier, A. T. Ngo, P. Bonville and M. P. Pileni, *J. Phys. Chem. B*, 2004, **108**, 1848.
14 Y. Lalatonne, L. Motte, J. Richardi and M. P. Pileni, *Phys. Rev. E*, 2005, **71**, 011404.
15 N. Kohler, C. Sun, A. Fichtenholtz, J. Gunn, C. Fang and M. Zhang, *Small*, 2006, **2**, 785–792.
16 P. C. Lin, P. H. Chou, S. H. Chen, H. K. Liao, K. Y. Wang, Y. J. Chen and C. C. Lin, *Small*, 2006, **42**, 485–489.
17 R. Lawaczec, H. Bauer, T. Frenel, M. Hasegawa, Y. Ito, K. Kito, N. Miwa, H. Tsutui, H. Vogler and H. J. Weinmann, *Acta Radiol.*, 1997, **35**, 584.
18 W. W. Yu, E. Chang, C. M. Sayes, R. Drezek and V. L. Colvin, *Nanotechnology*, 2006, **17**, 4483–4487.
19 F. Bertorelle, C. Wilhelm, J. Roger, F. Gazeau, C. Ménager and V. Cabuil, *Langmuir*, 2006, **22**, 5385–5391.
20 S. Verdaguer, M. Puerto Morales, O. Bomati-Miguel, C. Bautista, X. Zhao, P. Bonville, R. Perez de Alejo, J. Ruiz Cabello, M. Santos, J. Tendillo-Cortigo and J. Ferreiros, *J. Phys. D: Appl. Phys.*, 2004, **37**, 2054–2059.
21 N. Nitin, L. E. LaConte, O. Zurkiya, X. Hu and G. Bao, *J. Biol. Inorg. Chem.*, 2004, **9**(6), 706–12.
22 D. B. Robinson, H. H. Persson, H. Zeng, G. Li, N. Pourmand, S. Sun and S. X. Wang, *Langmuir*, 2005, **21**, 3096–103.
23 D. Portet, B. Denizot, E. Rump, F. S. Hindre, J. J. Le Jeune and P. Jallet, *Drug Dev. Res.*, 2001, **54**, 173–181.
24 D. Portet, B. Denizot, E. Rump, J. J. Le Jeune and P. Jallet, *J. Colloid Interface Sci.*, 2001, **238**, 37–42.
25 G. Baldi, D. Bonacchi, M. Comes Franchini, D. Gentili, G. Lorenzi, A. Ricci and C. Ravagli, *Langmuir*, 2007, **23**, 4026–4028.
26 P. Mowat, F. Franconi, C. Chapon, L. Lemaire, J. Dorat, F. Hindré, J. P. Benoit, P. Richomme and J. J. Le Jeune, *NMR Biomed.*, 2007, **20**, 21–27.
27 I. Fishbein, I. S. Alferiev, O. Nyanguile, R. Gaster, J. M. Vohs, G. S. Wong, H. Felderman, I.-W. Chen, H. Choi, R. L. Wilensky and R. J. Levy, *Proc. Natl. Acad. Sci. U. S. A.*, 2006, **103**, 159–164.
28 T. J. Martin and V. Grill, *Australian Prescriber, 6*, 2000, **23**, 130–132.
29 E. Gumienna-Kontecka, R. Silvagni, R. Lipinski, M. Lecouvey, F. C. Marincola, G. Crisponi, V. M. Nurchi, Y. Leroux and H. Kozlowski, *Inorg. Chim. Acta*, 2002, **339**, 111–118.
30 R. D. Peacock, *Struct. Bonding*, 1975, **22**, 83.
31 E. Podstawka, R. Borszowska, M. Grabowska, M. Drag, P. Kafarski and L. M. Proniewcz, *Surf. Sci.*, 2005, **599**, 207.
32 W. Gao, L. Dickinson, C. Grozinger, F. G. Morin and L. Reven, *Langmuir*, 1996, **12**, 6429.
33 F. Fredoueil, M. Evain, D. Massiot, M. Bujoli-Doeuff and B. Bujoli, *J. Mater. Chem.*, 2001, **11**, 1106–1110.
34 Y. Zhang, N. Kohler and M. Zhang, *Biomaterials*, 2002, 1553.